

The Portable 18 cm Submillimeter-wave Telescope (POST18)

Tomoharu Oka, Satoshi Yamamoto, Kazuhisa Kamegai, and Masaaki Hayashida

Department of Physics, Faculty of Science, The University of Tokyo, 7-3-1 Hongo, Bunkyo-ku, Tokyo 113-0033, Japan; tomo@phys.s.u-tokyo.ac.jp, yamamoto@phys.s.u-tokyo.ac.jp, kamegai@phys.s.u-tokyo.ac.jp, mahaya@phys.s.u-tokyo.ac.jp

Masafumi Ikeda

Computational Science Division, Advanced Computing Center, The Institute of Physical and Chemical Research (RIKEN), 2-1 Hirosawa, Wako, Saitama 351-0198, Japan; ikeda@atlas.riken.go.jp

and

Leonald Bronfman

Universidad de Chile, Departamento de Astronomia, Casilla 36-D, Santiago, Chile; leo@das.uchile.cl

ABSTRACT

We have developed a portable submillimeter-wave telescope to perform the wide-angle survey of the Milky Way in the $^3P_1-^3P_0$ line of the neutral carbon atom (C^0). An offset paraboloid main reflector with a diameter of 18 cm is employed. A superconductor-insulator-superconductor (SIS) mixer receiver is used to receive the 500 GHz band. An acousto-optical spectrometer which has the total bandwidth of 900 MHz has also been developed. We have performed a test operation at Pampa la Bola (alt.4800 m), Chile from September to October 2002. Atmospheric opacity was 0.5–0.9 at 492 GHz and the system noise temperature was 650–1000 K during the operation. We observed 10 representative sources in the southern sky, and detected the C^0 $^3P_1-^3P_0$ line from 4 sources.

1. INTRODUCTION

The interstellar medium is essentially composed of hydrogen, either in atomic or molecular form. The 21 cm line of atomic hydrogen HI was the principal tool used to study the interstellar medium and its large-scale distribution in the Galaxy. As for the molecular hydrogen, the symmetric H_2 molecule does not radiate in the radio wavelength, the asymmetric carbon monoxide (CO) molecule – the most abundant molecule after H_2 – provides a superior tracer of H_2 in interstellar space. Since the first detection of the CO $J=1-0$ line (Wilson et al. 1970), it has been principal tool used to study the molecular component in the Galaxy and extragalaxies.

Large-scale CO surveys (e.g., Gordon & Burton 1976; Sanders, Solomon, & Scoville 1984; Dame et al. 1987; Bronfman et al. 1988) have shown that most of molecular material in the Galaxy is contained in the form of molecular clouds, which are sites of star formation. The Galactic distribution of molecular clouds is characterized by their concentration in the Galactic center region and in a "ring" at a Galactocentric radius of 0.4–0.8 R_0 , in sharp contrast to the smooth HI distribution. In addition, large complexes of molecular clouds are concentrated to spiral arms in the Galactic disk (e.g., Despois & Baudry 1988; Clemens, Sanders, & Scoville 1988). These indicate that formation processes of molecular clouds must be related to the kiloparsec-scale Galactic structure.

To investigate the formation process of molecular

clouds, it is crucial to know the large-scale distribution and kinematics of molecular cloud forming regions in the Galaxy. First, direct observations of molecular cloud forming region must be essential. Neutral carbon atom (C^0) is the promising tool to trace molecular cloud forming regions, since chemical models predict that C^0 becomes abundant in the early stage of molecular cloud evolution (e.g., Suzuki et al. 1992). Recently, extensive survey of nearby molecular clouds in the C^0 $^3P_1-^3P_1$ line (492 GHz) with Mt. Fuji submillimeter-wave telescope found such molecular clouds in the early stage of chemical evolution (Maezawa et al. 1999; Kamegai et al. 2003). However, the sky coverage of the Mt. Fuji telescope survey is still limited (~ 40 square degrees), since its beamsize ($2.2'$ @492GHz) is too small to survey whole the Galaxy.

For the exclusive use of the wide-angle survey of the Milky Way in the C^0 $^3P_1-^3P_0$ line, we have developed a small submillimeter-wave telescope – the portable 18 cm submillimeter-wave telescope (POST18). This paper presents the descriptions of POST18, as well as the results of a test operation at Pampa la Bola, Chile.

2. INSTRUMENT

A schematic drawing of the telescope is shown in Figure 1. The parameters of the telescope are listed in Table 1. The telescope is designed to be portable. Total weight of the telescope, including receiver, backend, and control system, is approximately 150 kg.

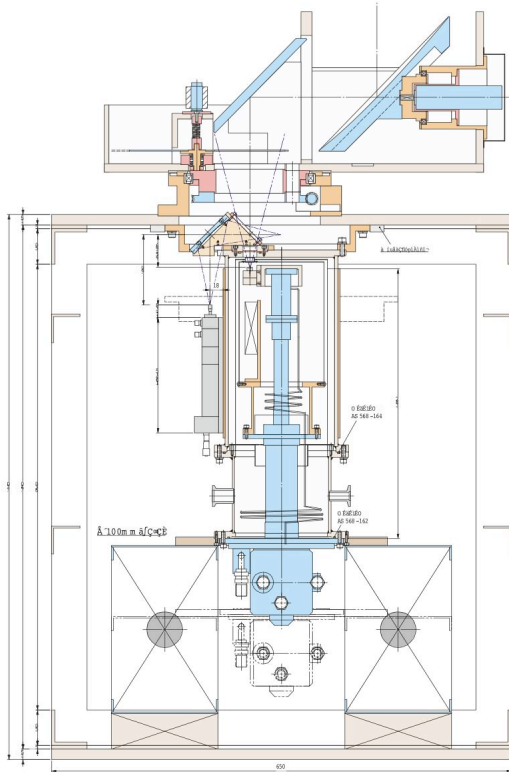


FIGURE 1. A schematic drawing of POST18.

TABLE 1. The parameters of POST18.

Parameter	Value
Main reflector	
Optics	offset paraboloid
Diameter	18 cm
Focal length	420 mm
Receiver	
Cryocooler	two-stage GM
Mixer type	SIS PCTJ
IF frequency	1.8–2.5 GHz
Receiver temperature	203 K
Spectrometer	
Type	AOS
Bandwidth	900 MHz
Channel number	1728 ch
Resolution	1.0 MHz

2-1. Antenna

We employed an offset paraboloidal mirror with the diameter of 18 cm as the main reflector. The focal length

of the main reflector was chosen to be as short as 420 mm for compactness. The beam from the main reflector is dropped by a flat sub-reflector, being directed to the mixer horn in the dewar.

Two same harmonic drive motors are used to drive azimuth and elevation axes. The torque of motors is 1.5 N m, and the maximum velocity is 84 rpm. Rotations of the motors are decelerated by 50:1 and 100:1 in Az and El, respectively. The Az axis is driven via a 160:1 worm gear. Mechanical micro switches are equipped for the both axes to determine the origins and limits.

2-2. Receiver

We developed a superconductor-insulator-superconductor (SIS) mixer receiver for 500 GHz band. We employed a Nb-based parallel connected twin junction (PCTJ) type mixer. The mixer is operated in the double sideband mode, and the 492 GHz signal is received in the lower sideband. The intermediate frequency (IF) is 1.8 to 2.5 GHz. DC bias (~ 1.6 mV) is applied to the mixer by a bias driver (Nitsuki) via a bias circuit. The Josephson current is suppressed by applying a magnetic field of 500–800 G. The field is generated by two permanent magnets.

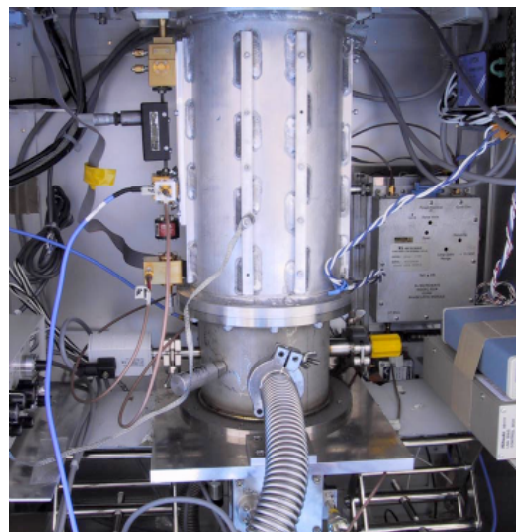


FIGURE 2. 500 GHz SIS mixer receiver.

The local oscillator (LO) signal is generated by multiplying the output of a W-band (~ 80 GHz) Gunn diode oscillator with a 2x2 multiplier (RPG). The LO power (~ 1 mW) is adjusted by a mechanical attenuator. The LO frequency is stabilized to a synthesized signal generator (Agilent) by a phase-locked loop. Line frequencies from celestial objects are tracked to by adjusting the frequency of the signal generator. The LO signal is quasi-optically coupled to the radio frequency (RF) signal by free-standing wire grid equipped on the top of the dewar.

The receiver employs a two-stage Gifford-MacMahon cryocooler, which has cooling capacity of 0.1 on the 4 K cold stage with a 1.5 kW power consumption (Sumitomo

RD101). The receiver dewar is evacuated to 10^{-4} Torr before cooling. It takes 10 hours to cool the mixer from room temperature to the operation temperature (~ 4 K).

The IF signal from the mixer was amplified by a cooled low noise amplifier (LNA, Nitsuki 9838S4). The LNA is composed of 3 GaAs high electron mobility transistors (HEMTs). The operation temperature of the LNA is ~ 15 K. The receiver noise temperature including LNA was 203 K in DSB.

2-3. Backend

The IF signal from the dewar is amplified by +66 dB at room temperature, and is fed into a wideband acousto-optical spectrometer (AOS). A Bragg cell made by GEC Marconi was used as a modulator. The imaging optics enables us to cover 900 MHz bandwidth with a 1728 channel charge coupled device (CCD) array. The effective frequency resolution of the spectrometer is 1.0 MHz. The frame rate of the CCD was set to 4 ms. The gain variation of a spectrum obtained with the AOS is less than 3 dBp-p over 700 MHz.

2-4. Control System

All instruments are controlled by a personal computer via GP-IB and digital I/O interfaces. The operating system is Windows 2000. The telescope control software has been developed with the Visual C++ package.

3. PERFORMANCE

On September 16th 2002, the telescope was installed at Pampa la Bola (alt. 4800 m), Chile. We used the facility of the Atacama Submillimeter-wave Telescope Experiment (ASTE). The electric power was supplied from the ASTE power plant. We evaluated the telescope performance before test observations.



FIGURE 3. POST18 installed at Pampa la Bola.

3-1. Optical Pointing

The instrumental pointing errors are measured by

observing stars with an optical telescope attached to the main reflector. The errors are removed by fitting measured deviations to the following equations with seven parameters (x_1 - x_7):

$$\begin{aligned} dAz &= -x_1 \cos(x_2 - Az) \tan(EI) + x_3 \tan(EI) \\ &\quad + x_4 / \cos(EI) + x_5 \\ dEI &= -x_1 \sin(x_2 - Az) + x_6 EI + x_7 \end{aligned}$$

where dAz and dEI are deviations in real angle. The residuals of the fitting are $70''$ both in Az and EI .

3-2. Radio Pointing

After the optical pointing, the pointing errors of radio axis are measured by observing continuum emission from the sun and the moon. During the test operation, pointing accuracy was maintained to $75''$ in rms.

3-3. Beam Efficiency

The beam efficiency was measured by observing the full moon. The efficiency (\square_{moon}) was estimated with large uncertainty ($\sim 15\%$), to be 0.85 by assuming the brightness temperature of the new moon to be 110 K.

3-4. Atmospheric Transmission

The atmospheric opacity was measured by tipping the main reflector around the EI axis. The zenith opacity at 492/496 GHz was from 0.5 to 1.0 during the operation.

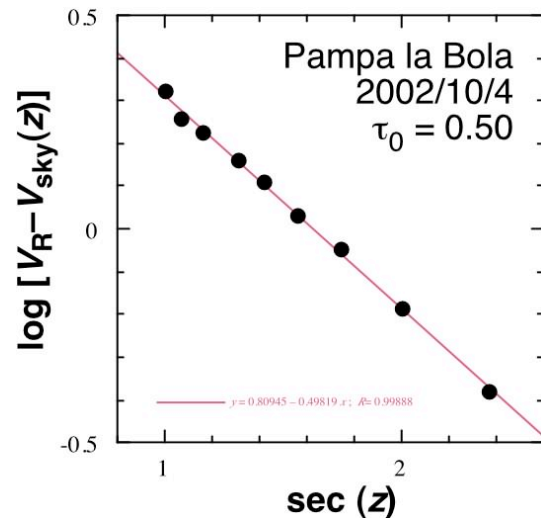


FIGURE 4. An example of opacity measurement.

4. TEST OBSERVATIONS

Test observations are conducted over a short period of ~ 1 week. We observed 10 representative sources in the southern sky (\square -Oph, NGC6334, \square -Carina, Southern Coal Sack, Sgr B, Corona Australis, NGC2024, M17, Lupus Cloud, Sgr A), and detected the $C^0 \ ^3P_1 - ^3P_0$ line from 4 sources. (\square -Oph, NGC6334, M17, NGC2024). Followings are brief discription of the results of

NGC6334 and M17.

4-1. NGC6334

NGC6334 is an active star forming region with $L_{\text{FIR}}=1 \times 10^6 L_{\text{solar}}$. We performed a mapping observations toward NGC6334. 28 $\text{C}^0 \ ^3\text{P}_1\text{-}^3\text{P}_0$ spectra with a $10'$ grid spacing covering a $1^\circ \times 1^\circ$ area were obtained in the position-switching mode. Typical on-source integration time was ~ 600 sec.

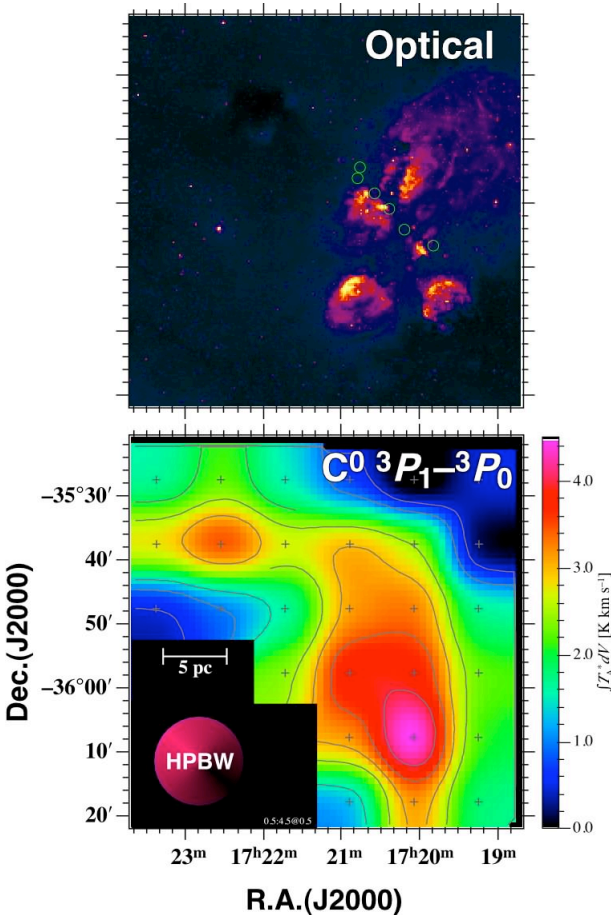


FIGURE 5. Map of $\text{C}^0 \ ^3\text{P}_1\text{-}^3\text{P}_0$ line emission integrated over $V_{\text{LSR}}=-10$ to $+20 \text{ km s}^{-1}$ with an optical image of the same area.

4-2. M17

M17 is an active star forming region with $L_{\text{FIR}}=4 \times 10^6 L_{\text{solar}}$. We obtained a $\text{C}^0 \ ^3\text{P}_1\text{-}^3\text{P}_0$ spectrum toward the emission peak, which is suggested by the Mt. Fuji telescope survey. The on-source integration time was 256 sec.

The spectrum is characterized by an intense main component at $V_{\text{LSR}}=20 \text{ km s}^{-1}$ and high-velocity wing features in both sides. Follow-up observations with Mt. Fuji submillimeter-wave telescope revealed that the blue-shifted wing emission comes from small area, while the red-shifted wing emission extends over $1 \text{ deg} \times 1 \text{ deg}$. This red-shifted wing emission could belong to a new

population of neutral interstellar matter in the Galaxy.

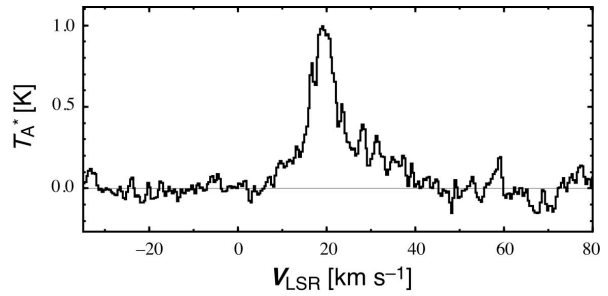


FIGURE 6. A $\text{C}^0 \ ^3\text{P}_1\text{-}^3\text{P}_0$ spectrum toward M17.

5. CURRENT STATUS

These preliminary results demonstrate the strong points of POST18: (1) efficient survey ability, (2) high sensitivity to spatially extended, faint emission. These characteristics are essential to perform a wide-angle survey of the Galaxy.

After the test operation at Pampa la Bola, the telescope has been disassembled and sent back to Tokyo. We are fixing the problems encountered during the operation, and preparing for the next operation at the site. Some improvement on the system has been done: reducing the receiver noise temperature to $T_{\text{RX}}=138 \text{ K}$, improving the tracking accuracy, and reducing digital noise in the signal averager.

REFERENCES

- Bronfman, L., Cohen, R. S., Alvarez, H., May, J., & Thaddeus, P. 1988, *ApJ*, 324, 248
 Clemens, D. P., Sanders, D. B., & Scoville, N. Z. 1988, *ApJ*, 327, 139
 Dame, T. M., Ungerechts, H., Cohen, R. S., de Geus, E. J., Grenier, I. A., May, J., Murphy, D. C., L.-A. Nyman, & Thaddeus, P. 1987, *ApJ*, 322, 706
 Despois, D., & Baudry, A., 1988, *A&A*, 195, 93
 Gordon, M. A., & Burton, W. B. 1976, *ApJ*, 208, 346
 Kamegai, K., Ikeda, M., Maezawa, H., Ito, T., Iwata, M., Sakai, T., Oka, T., Yamamoto, S., Sekimoto, S., Tatematsu, K., Noguchi, T., Saito, S., Fujiwara, H., Ozeki, H., Inatani, J., & Ohishi, M. 2003, *ApJ* inpress
 Maezawa, H., Ikeda, M., Ito, T., Saito, G., Sekimoto, Y., Yamamoto, S., Tatematsu, K., Arikawa, Y., Aso, Y., Noguchi, T., Shi, S.-C., Miyazawa, K., Saito, S., Ozeki, H., Fujiwara, H., Ohishi, M., & Inatani, J. 1999, *ApJ*, 524, L129
 Suzuki, H., Yamamoto, S., Ohishi, M., Kaifu, N., Ishikawa, S., Hirahara, Y., & Takano, S. 1992, *ApJ*, 392, 551
 Wilson, R. W., Jefferts, K. B., & Penzias, A. A. 1970, *ApJ*, 161, L43
 Sanders, D. B., Solomon, P. M., & Scoville, N. Z. 1984, *ApJ*, 289, 373